

Simulating Galaxy Evolution

Joseph Silk and Rychard Bouwens

Departments of Astronomy and Physics, and Center for Particle Astrophysics, University of California, Berkeley, CA 94720

Abstract. The forwards approach to galaxy formation and evolution is extremely powerful but leaves several questions unanswered. Foremost among these is the origin of disks. A backwards approach is able to provide a more realistic treatment of star formation and feedback and provides a practical guide to eventually complement galaxy formation *ab initio*.

INTRODUCTION

Understanding how galaxies formed is the key to unraveling the mysteries of the high redshift universe. To interpret the deepest images of distant galaxies one has to simulate galaxy evolution. The prescription for such a simulation seems straightforward. Take a gas cloud, massive enough to be self-gravitating, and add a simple prescription for star formation based on the local free-fall time scale. In practice, this approach has yielded star formation histories that appear to match observations.

However the predictive power of this approach is limited. The reason is the following. One has to assume a prescription for star formation. Reasonable guesses can be made, but one has no guarantee that these are valid. There is no way of evaluating the uncertainty in the adopted ansatz for forming stars. This is true for primordial clouds, and equally valid for current star formation. Of course the star formation prescription, once selected, has parameters that can be adjusted, often with little freedom when confronted with the observational data. This approach has been applied to the early universe, commencing with density fluctuations that grow by hierarchical clustering of cold dark matter.

One can try to assess the uncertainties by comparing snapshots of the universe at different redshifts. If one matches the data, one can deduce that one has a working model of galaxy formation, but one cannot expect this to be a useful guide to extreme situations that are not included in the simple algorithm. These might include, for example, the role of active galactic nuclei in primordial and current epoch star formation. I conclude that it is useful to consider an alternative to “*ab initio*” galaxy formation. In this talk I will describe such an approach that is based

on nearby examples of star formation in a global context, that one attempts to run backwards in time. Clearly, forwards and backwards evolution are complementary descriptions of the same fundamental issues that describe galaxy formation.

GALAXY EVOLUTION FROM PRIMORDIAL FLUCTUATIONS

Inflationary cosmology prescribes the initial spectrum of density fluctuations. The horizon scale at matter-radiation equality imprints a scale on the relic fluctuation spectrum: at $L \gg L_{eq} \simeq 12(\Omega h^2)^{-1}$ Mpc, $\delta\rho/\rho \propto M^{-1/2-n/6}$ and $n \approx 1$ whereas at $L \ll L_{eq}$, n_{eff} approaches -3 , reflecting scale invariance for fluctuations that entered the horizon during radiation domination. On galaxy scales, $n_{eff} \approx -2$. This leads to a hierarchical formation sequence of structure. Larger and larger structures merge together. Numerical simulations show that some substructure survives.

This is potentially a problem for understanding why galactic disks remain thin if the surrounding dark halos contain even a percent of their mass in massive substructures, characteristic in mass, say, of dwarf galaxies. Dwarf-disk interactions would overheat the disk [19]. This can be partially rectified by gas infall, which certainly helps renew thin disks. The discovery of high velocity hydrogen clouds at the periphery of the halo lends some support to the availability of a gas reservoir today [1].

The properties of dark halos are accounted for by hierarchical clustering. The abundance, mass function, density profile and rotation curve for a typical galaxy halo all agree with empirical estimates. The clustering of galaxies is described by the galaxy correlation function, and simulations of clustering provide a fit over several decades of scale. One accounts for the mass function of galaxy clusters and its evolution with redshift [2,3] by setting $\Omega \approx 0.3 (\pm 1)$. Interpretation of massive halos as rare peaks accounts for the observed clustering of Lyman break galaxies at $z \sim 3$ [4].

The properties of the intergalactic medium agree with predictions of the hierarchical model. One has to adopt a metagalactic ionizing radiation field. This is taken from the observed quasar luminosity function. The gas distribution from the simulations is exposed to the ionizing radiation field, and the effects of the peculiar velocity field are found to play an important role in reproducing Lyman alpha cloud absorption profiles. One can explain [5] the distribution of observed column densities ranging from damped Lyman alpha clouds with HI column densities in excess of 10^{21} cm⁻² down to the Lyman alpha forest below 10^{14} cm⁻². The gas overdensities range from $\delta\rho/\rho$ of order several hundred for damped clouds to unity for the forest. The structural properties of the Lyman alpha clouds are simply understood. There is some controversy however over the nature of the relatively rare damped clouds. These have been argued to be rotating protodisks [6]. However the observed spread of velocities is not simply a thin disk, but can either be

interpreted as a thick disk or as a more incoherent, quasi-spherical halo containing many smaller clouds [7].

More problematic for disk theory is the failure of simulations to reproduce the sizes of galactic disks. Angular momentum conservation of a uniformly collapsing and dissipating cloud of baryons within a dark halo suggests that the disk size is λR_i , where R_i is the halo virialization radius and λ is the critical dimensionless angular momentum. One has $\lambda \approx 0.06$ and R_i is typically about 100 kpc. This argument would actually give the correct disk size. However the clumpy nature of the halo is found to drive efficient angular momentum transfer via dynamical friction. The disk size found in simulations is a factor of five or more smaller than observed disk scale lengths [8]. Evidently feedback from star formation is conspiring to limit the collapse of the gas.

The galaxy luminosity function also represents a challenge for theoretical models, which more naturally specify the galaxy mass function. There are two difficulties. At the low mass end, the predicted slope of the mass function ($dN/dm \approx m^{-2}$) is a poor fit to the power-law tail of the galaxy luminosity function, the slope of which depends on galaxy color selection and varies between $dN/dL \approx L^{-3/2}$ in the blue and $dN/dL \approx L^{-1}$ in the red. One corrects this problem by introducing inefficient star formation in low mass potential wells. The fraction of gas forming stars is assumed to be $(\sigma/\sigma_{cr})^\alpha$, with $\alpha \approx 2$, where $\sigma_{cr} \approx 75 \text{ km s}^{-1}$ denotes the transition velocity dispersion, below which retention of interstellar gas energised by supernova-driven winds becomes suppressed. This assumes that supernovae are effective at disrupting the interstellar gas in the shallow potential wells characteristic of dwarf galaxies [9]. However the efficiency may only be high at masses below $\sim 10^6 M_\odot$, according to a recent analysis of starbursts in dwarf galaxies [10]. This would only flatten the luminosity function at very low luminosities if one counts all gas-retaining galaxies. One difference between dwarfs ($\lesssim 10^8 M_\odot$) and giants is that the supernova ejecta are expelled, so that the residual gas, if retained, is very metal-poor. This might be sufficient to reduce the efficiency of star formation sufficiently so as to produce a population of low surface brightness dwarfs.

At high luminosities the challenge is to explain why the nonlinear clustering mass present is $\sim 10^{14} M_\odot$ whereas the value of L_* , above which the number of galaxies decreases exponentially, is $10^{10} h^{-2} L_\odot$. The corresponding dark halo mass is around $10^{12} M_\odot$. Evidently some physical effect is intervening to limit the luminosity of a galaxy, which does not track the mass of the dark potential wells. The generally accepted resolution is that baryonic cooling is a necessary condition for star formation to occur in a primordial contracting cloud. If the density is too low for gas cooling, the intergalactic gas remains hot and diffuse. Efficient star formation must occur within a dynamical time-scale. This is certainly how monolithic formation of an elliptical must have occurred. In this case, the condition that the gas cooling time be less than a collapse time sets a maximum value on cooled galaxy baryon mass of about $10^{12} M_\odot$.

However gas continues to accrete and cool. The total mass of cooled gas does not provide a distinctive cut-off in the mass function of baryons [11]. One has to vary

the efficiency of star formation, reducing it on time-scales longer than a dynamical time, in order to account for L_* . One can appeal to cluster formation to heat up the intergalactic gas, thereby removing the reservoir of cold gas which would potentially be accreted. This would lead one to expect that cluster ellipticals have a relatively homogeneous distribution of formation times, peaked at the epoch of cluster formation. One has to assume a hot gas environment for field ellipticals, associated with galaxy groups, to restrict cold gas infall. However since clustering in the field develops more recently than for rich clusters one expects field ellipticals, on the other hand, to display a much broader range of ages, and reveal, in some cases, signs of recent or current infall. Indications of this effect can be seen in the enhanced scatter in the fundamental plane for field ellipticals relative to cluster ellipticals [12].

For disk galaxies, the comparison of mass and luminosity via the predicted mass function challenges interpretations of the Tully-Fisher correlation between luminosity and maximum rotation velocity [13]. The observed dispersion of fifteen percent in inferred distance [14] may be compared with the dispersion between mass and halo circular velocity in the CDM hierarchy, which is of order 100 percent. Implementation of a prescription for star formation can reduce the dispersion between cooled baryon mass, and hence luminosity, and disk rotational velocity to the observed range by, for example, allowing stars to preferentially form in the more massive disks where the baryons are self-gravitating and dense enough to suppress supernova-driven winds. However there is a price: the Tully-Fisher normalization yields the disk mass-to-luminosity ratio, and the CDM hierarchy inevitably favors a high value relative to the observed value of $M/L \sim 10 h$ for the baryon-dominated regions of disks.

GALAXY EVOLUTION VIA REVERSE ENGINEERING

A complementary approach to galaxy evolution allows one to circumvent some of these difficulties, although at the risk of introducing other complications. One commences with nearby galaxies, develops a model for star formation, and evolves the galaxies backwards in time. Actual images or idealized models of nearby galaxies are used as the starting point. Suppose one first ignores dynamical evolution. Star formation in disks can be described by an expression of the form

$$\text{SFR} = \epsilon \mu_{\text{gas}} \Omega(r) f(Q).$$

Here μ_{gas} is the surface density of atomic and molecular gas, $\Omega(r)$ is the rotation rate, Q is the Toomre parameter (approximately given for a self-gravitating disk of gas by $\frac{\kappa\sigma}{\pi G\mu_{\text{gas}}}$, where κ is the epicyclic frequency and σ is the gas velocity dispersion) that guarantees gravitational instability to axisymmetric perturbations if $Q < 1$, and ϵ is an efficiency parameter. One needs to generalize the dependence on Q to allow for non-axisymmetric instabilities, such as density waves which are responsible for the growth of molecular clouds and for the gravitational contribution of the

stellar component. In general, however, one expects there to be a threshold for local instabilities when the surface density drops below a critical value, for typical disks amounting to about $\mu_{\text{gas}} \approx 10 M_{\odot} \text{pc}^{-2}$. This empirical expression fits global star formation rates in disks remarkably well [15], and ϵ may be interpreted as the fraction of gas converted into stars per dynamical time. Infall is one remaining ingredient that needs to be added.

For individual disks, this model has been exploited to demonstrate that disks form inside out, that disk surface brightness increases by almost a magnitude [16] to $z \sim 1$, and to account for the chemical evolution of old disk stars and of the interstellar medium at high redshift [17]. The model has considerable potential for predicting how galaxies appear to evolve in deep images obtained of the distant universe. In fact, one study [18] has already demonstrated that such a scaling in galaxy size is necessary to reconcile faint galaxies sizes with galaxies at low redshift, this study carefully considering changes in the pixelisation, the PSF, and the surface brightness relative to the noise. Of course, a careful consideration of many of the same effects is important for testing models against the observations. One has to add a disk formation epoch, chosen from an analytical prescription for hierarchical CDM cosmology and some evolution in number density. The latter is required to crudely account for merging and is necessary to reproduce the observed deep galaxy counts. Ellipticals and spheroids must also be incorporated into the model. While these systems do not dominate the number counts, which at faint magnitudes are dominated by disks and their irregular precursors, they are important in the cumulative star formation history of the universe. Approximately half of the mass in stars is in the spheroidal component, and hence mostly in E's and S0's. This is the approximate assessment for the local luminosity function (and is due to the fact that while ~ 30 percent of galaxies are E's and S0's, the associated M/L is about twice as large as for typical spirals). One also reaches an independent verification of this from the cosmic far infrared background. This recently discovered diffuse flux at $100 - 300 \mu\text{m}$ amounts to $\lambda i_{\nu} \approx 20 \text{ nW/m}^2/\text{s}^2$, comparable to the diffuse optical light flux when integrated over the HDF and near infrared. Modelling of disk galaxies incorporating dust can reproduce the optical background but only about fifty percent of the FIR background is explained by optically visible systems. The remainder is presumed to be due to dusty ellipticals. Of course if these systems form stars at an early epoch z_E relative to spirals at z_S , then the inferred mass in stars (for the same initial mass function) in dust enshrouded spheroids is equal to $[(1 + z_E)/(1 + z_S)]$ times the contribution from disks. This comparison suggests that $z_E \sim z_S$ though in principle one could have $z_E \gg z_S$.

One might worry that the FIR background could be due to AGN. However modelling of the x-ray background effectively constrains the AGN contribution to diffuse hard photons. Compton self absorption of the x-rays, required to obtain a spectral fit of the XRB, limits the possible contribution to the diffuse FIR background by dust-shrouded, x-ray-emitting AGN to be almost ten percent of the observed background. Direct observations by SCUBA find ultraluminous galaxies at $z = 1 - 3$. Perhaps ten percent of these may be AGN-powered according to the previous

argument, and this is consistent with direct spectroscopic signatures.

Disk Parameterisation

There are two major uncertainties in the modelling of the disk star formation rate: infall and efficiency. One can constrain the role of infall by three independent methods that respectively appeal to chemical evolution, disk dynamics, and to the evolution of disk sizes. The best studied is chemical evolution. Infall of metal-poor gas into the early gas is required to account for the paucity of metal poor G dwarfs. The sharp decline in supersolar metallicities of disk stars means that recent metal-poor infall is greatly reduced relative to infall in the first 5 Gyr. Infall of gas-rich clumps is predicted in the CDM model, but these interactions must avoid overheating the disk. Less than 4% of the disk can have fallen in over the past 5 Gyr according to one study [19]. However recent calculations suggest that infalling satellites preferentially tilt rather than heat the disk [20]. The implications for high redshift galaxies is that disks are small at $z > 1$. Without infall, disks would not be sufficiently small, according to one recent analysis, to account for the decrease in faint galaxy angular diameter.

One can only decompose disks from bulges to $z \lesssim 1$, using HST data. Evolution of disk sizes to this redshift is quite model-dependent. Disk size varying as $(1+z)^\alpha$, with $\alpha \approx 2$, fits the available data. However selection biases need to be modelled more carefully. One selects earlier type galaxies at high redshift than at low redshift because of surface brightness dimming, and this complicates comparisons.

Disk Physics

The essence of disk formation lies in inefficiency. Galaxies retain a sufficient gas reservoir so as to still be vigorously forming stars at the present epoch. The star formation rate increases dramatically with cosmic epoch, possibly peaking near $z \sim 2$. Hence gas infall drops off dramatically. This also is implicit in models of galactic chemical evolution, where infall of metal-poor gas over the first five or so Gyr helps account for the metal distribution of old disk stars. The inefficiency of star formation must be due, not to the availability of a gas supply but rather arises from being controlled by disk physics.

Feedback of energy and momentum from star formation and death necessarily play an important role. One needs to include such physics to understand disk sizes. One could simultaneously account for gas longevity. Angular momentum transfer is central to such a model. A general class of theories which can successfully reproduce disk profiles is based on contracting viscous self-gravitating disks. The viscosity arises from cloud-cloud collisions, the cold disk being gravitationally unstable to cloud formation. The disk forms as angular momentum is transferred on a viscosity timescale. Since cloud collisions and mergers are assumed to drive star formation,

one naturally relates the star formation and viscosity time scales. An exponential surface density profile is naturally generated [21].

Bulge Evolution

Bulges are expected to be prominent in observations of high redshift galaxies, both because of disk evolution and the high bulge surface brightness. Yet the sequence of bulge formation is poorly understood, and this makes it difficult to formulate and test *ab initio* predictions of disk evolution. Consider the following alternatives. Bulges form before disks, either monolithically or in major (i.e. comparable, or at least mass ratio 1:10) mergers. Bulges form simultaneously with disks via satellite mergers. Bulges form after disks, via secular instability of disks, and bar formation followed by dissolution as gas inflow drives bulge formation [22]. Any of these scenarios are possible. Two, or even all three, may be operative. For example, secular evolution can form small bulges but not the massive objects of early type galaxies. Observational evidence that bulge and disk scale lengths are correlated favors a secular evolution origin of bulges for late-type spirals [23]. The ubiquity of bars, which are efficient at torquing accreting gas and driving the gas inwards to form a central bulge, also suggests that secular evolution must have played a significant role in bulge formation. Conversely, massive bulges are most likely formed by mergers. Satellite infall of gas-rich dwarf galaxies is expected to be a common occurrence in hierarchical models and provides a natural mechanism for simultaneously forming the bulges, as the dense stellar cores sink into the center of the galaxy by dynamical friction, and feeding disk growth with gas infall. There are hints of monolithic bulge formation from observations of many compact Lyman break galaxies, which have high star formation rates.

One can try to address this confusing range of bulge formation possibilities by examining the properties of disk galaxies at $z \lesssim 1$, where component separation into bulge and disk is possible at HST resolution. Late-forming bulges are inevitably bluer and smaller than early-forming bulges, at a given redshift. Figure 1 shows a comparison of the model predictions with available data. HST images are shown, in a comparison with the HDF. Analyses of similar images [24] show that only with larger samples at $z \sim 1$ could one be able to distinguish between alternative models of bulge formation.

LOOKING TO THE FUTURE

It will be possible in the not too distant future to greatly refine the observational constraints relevant to galaxy evolution. In Figure 2 we show HST Advanced Camera (2000) and NGST (2007) simulations of the same 85" x 85" field using the secular evolution scheme for bulge formation. The Advanced Camera simulations consider a 150,000-s integration, utilise a pixel size of 0.05 arcsec, and probe the *gri* optical bands to $i_{AB} \sim 30.3$, whereas the NGST simulations consider a similar

150,000-s integration, utilise a pixel size of 0.029 arcsec, and probe the 1,3,5- μm wavelength bands to $m_{1\mu\text{m},AB} \sim 31.6$. For comparison, we also show WFPC2 (pixel size is 0.1 arcsec, probes the I_{F814W} , V_{F606W} , and B_{F450W} bands to a limiting magnitude $I_{F814W,AB} \sim 29$) and NICMOS (pixel size is 0.2 arcsec, probes the J_{F110W} and H_{F160W} infrared bands to $H_{F160W,AB} \sim 28.3$) simulations. Since the fiducial secular model for bulge formation breaks down at high redshift, we have included a variation of the Pozzetti, Bruzual, & Zamorani [25] luminosity evolution model at these redshifts. The simulations include both K and evolutionary corrections, cosmological angular size relations and volume elements ($\Omega = 0.15$, $h = 0.5$), appropriate pixelisation, PSFs, and noise (see [18] for a discussion).

Obviously, one of the principal advantages of the Advanced Camera and NGST over WFPC2 and NICMOS are their increases in limiting magnitude, angular resolution, and field of view. Regarding the differing limiting magnitudes, using the Advanced Camera for similar length exposures to those shown here, one could probe to unobscured star formation rates $\sim 0.5M_{\odot}/\text{yr}$ at $z \sim 5$ whereas with WFPC2, the limiting rate is only $\sim 2M_{\odot}/\text{yr}$. For higher redshift observations, such as are only possible with NICMOS or NGST, NGST promises to push the sensitivity on unresolved star formation from its current value $\sim 20M_{\odot}/\text{yr}$ at $z \sim 10$ obtainable with NICMOS exposures down to $\sim 1M_{\odot}/\text{yr}$.

REFERENCES

1. Blitz, L. et al. 1998, preprint, astro-ph/9803251.
2. Eke, V. et al. 1998, MNRAS, 298, 1145.
3. Bahcall, N. and Fan, X. 1998, ApJ, 504, 1.
4. Giavalisco, M. et al. 1998, ApJ, 503,543.
5. Katz, N. et al. 1996, ApJ, 457, 57.
6. Wolfe, A. M. and Prochaska, J. 1998, ApJ, 507, 113.
7. Haehnelt, M., Steinmetz, M. and Rauch, M. 1998, ApJ, 495, 647.
8. Steinmetz, M. and Muller. E. 1995, MNRAS, 276, 549.
9. Dekel, A. and Silk, J. 1986, ApJ, 303, 39
10. Maclow, M. and Ferrara, A. 1998, preprint, astro-ph/9801237.
11. Thoul, A. and Weinberg, D. 1996, ApJ, 465, 608.
12. Forbes, D., Ponman, T. and Brown, R. 1998, ApJ, 508, L43.
13. Steinmetz, M. and Navarro, J. 1998, preprint, astro-ph/9808076.
14. Willick, J. 1998, preprint, astro-ph/9809160.
15. Kennicutt, R. 1998, ApJ, 498, 541.
16. Bouwens, R., Cayon., L. and Silk, J. 1997, ApJ, 489, L21.
17. Prantzos, N. and Silk, J. 1998, ApJ, 507, 229.
18. Bouwens, R., Broadhurst, and Silk, J. 1998, ApJ, 506, 557.
19. Toth, G. and Ostriker, J. P. 1993, AJ, 389, 5.
20. Huang, S. and Carlberg 1997, ApJ, 480, 503.
21. Lin, D. and Pringle, J. 1987, ApJ, 320, L87.
22. Norman, C., Sellwood, J. and Hasan, H. 1996, ApJ, 462, 114.

23. Courteau, S., R. de Jong and de Broeils, A. 1996, ApJ, 457, L73.
24. Bouwens, R., Cayon., L. and Silk, J. 1999, ApJ, in press, astro-ph/9812193.
25. Pozzetti, L., Bruzual, G., and Zamorani, G. 1996, MNRAS, 274, 832.

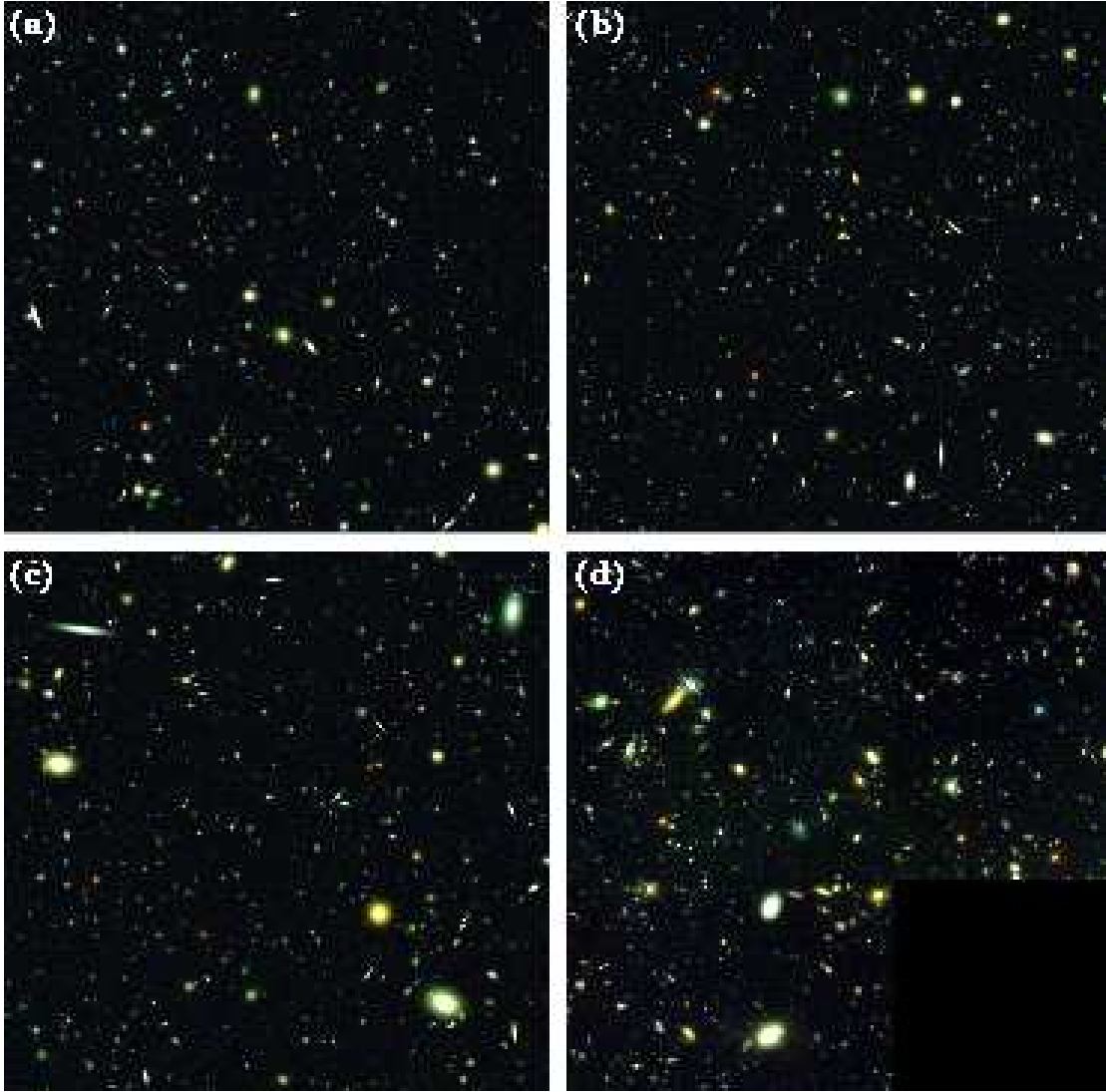


FIGURE 1. Comparison of simulated BVI images of a $2'' \times 2''$ patch of the HDF with the observed images (panel d). Panel (a) illustrates our secular evolution model for bulges, panel (b) illustrates our simultaneous formation model, and panel (c) illustrates our early bulge formation model. Calculations are performed using a galaxy-evolution software package written by one of the authors.

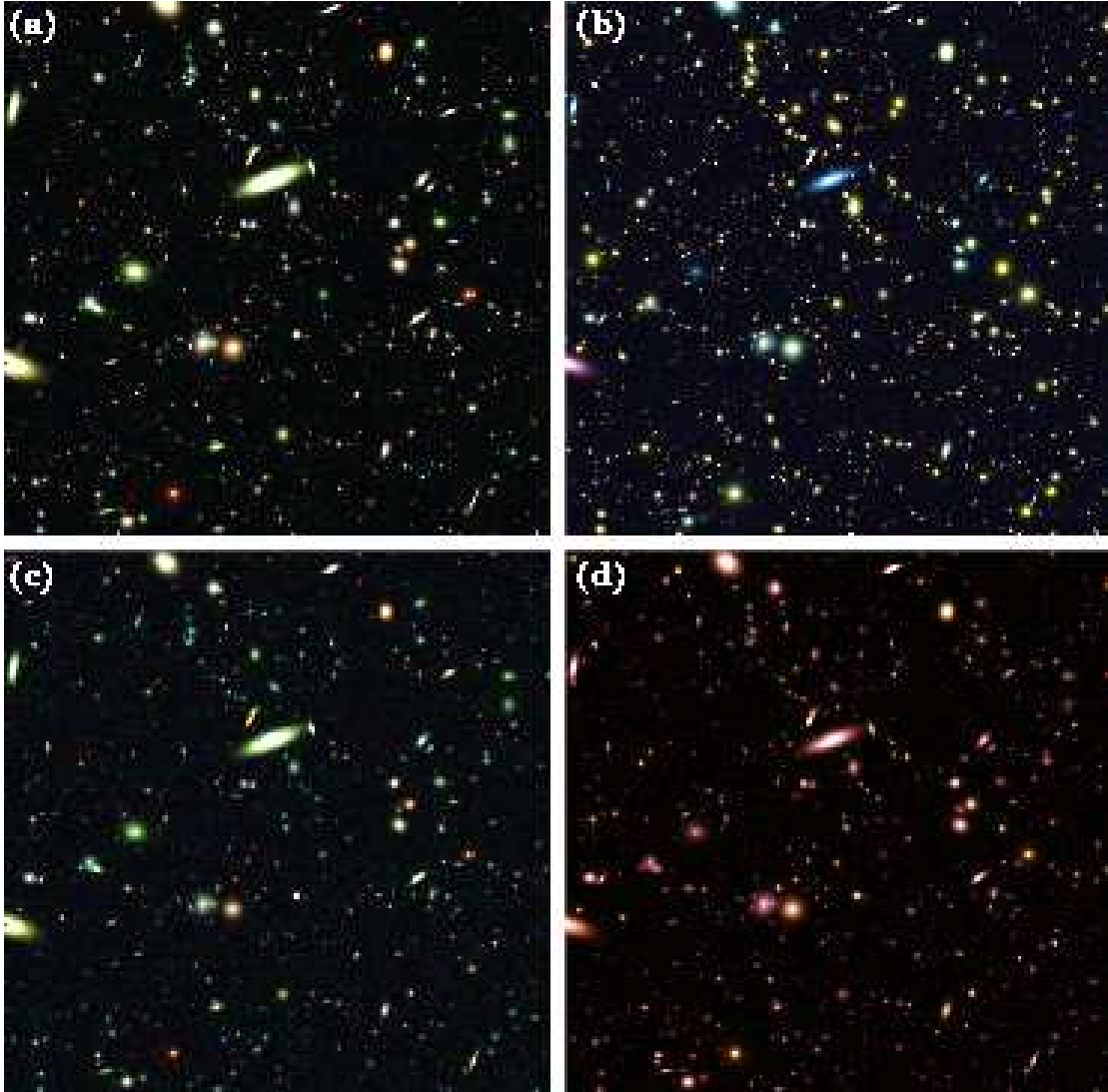


FIGURE 2. Simulated images of a $85'' \times 85''$ field using a secular evolution model for disks to $z = 1$ and the Pozzetti, Bruzual, & Zamorani luminosity evolution model for $z > 1$. Shown are 30-orbit *gri* exposures for the HST Advanced Camera (a), 150000-s $1,3,5\text{-}\mu\text{m}$ exposures for NGST (b), 30-orbit *BVI* exposures for HST WFPC2 (c), and 30-orbit *JH* exposures for the HST NIC3 camera (d). Calculations are performed using a galaxy-evolution software package written by one of the authors.